
Supplemental Data

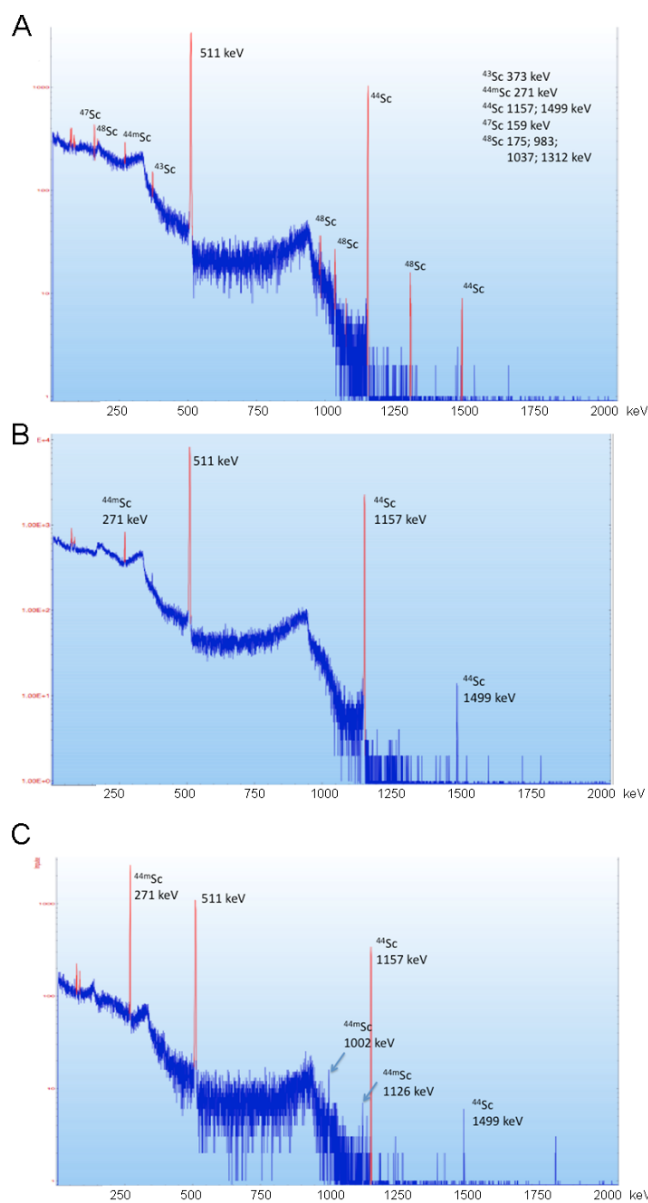
1. γ -Ray Spectrometry of Irradiated ^{44}Ca -Targets

Purpose. To produce ^{44}Sc via the $^{44}\text{Ca}(p,n)^{44}\text{Sc}$ -nuclear reaction at a cyclotron, targets that contain either natural calcium ($^{\text{nat}}\text{Ca}$, mixture of Ca-isotopes) or enriched calcium (^{44}Ca) can be irradiated (1-4). In order to investigate the difference among these possibilities we analyzed the composition of radioactive isotopes upon irradiation of targets composed of either $^{\text{nat}}\text{CaCO}_3$ or $^{44}\text{CaCO}_3$.

Experimental. For preparation of the targets, $^{\text{nat}}\text{CaCO}_3$ (200 mg, purum p.a., Fluka AG) or $^{44}\text{CaCO}_3$ (5-10 mg, 97.0%, Trace Sciences International) combined with graphite powder (150 mg, 99.9999%, Alfa Aesar) was pressed by a target press device and encapsulated in aluminum. Targets were irradiated for 30-40 min at the cyclotron facility at PSI using a proton energy of 17.6 ± 1.8 MeV and a beam current of 50 μA . Next, the irradiated CaCO_3 -targets were dissolved in 3 M HCl. Five hours (and 48 h) after the end of the irradiation (end of beam) aliquots of 1 mL were taken and analyzed by γ -ray spectrometry using an N-type high-purity germanium (HPGe) coaxial detector (EURISYS MESURES) and the Ortec InterWinner 5.0 software to determine the amount of ^{44}Sc and co-produced radioisotopes.

Results and Conclusion of the γ -Spectrometry. Because of the natural abundances of calcium isotopes in $^{\text{nat}}\text{Ca}$ (^{40}Ca : 96.94%; ^{42}Ca : 0.65%; ^{43}Ca : 0.14%, ^{44}Ca : 2.09%; ^{46}Ca : 0.004%; and ^{48}Ca : 0.19%) irradiation of $^{\text{nat}}\text{CaCO}_3$ -targets resulted in the production of ^{44}Sc along with other Sc-radioisotopes (^{43}Sc , 4%, $t_{1/2} = 3.89$ h; $^{44\text{m}}\text{Sc}$, 0.7%, $t_{1/2} = 58.6$ h; ^{47}Sc , 0.7%, $t_{1/2} = 80.4$ h; and ^{48}Sc , 0.7%, $t_{1/2} = 43.7$ h) as shown on the γ -spectrum obtained from aliquots of dissolved $^{\text{nat}}\text{CaCO}_3$ -target material upon irradiation (Supplemental Fig. 1A). The γ -spectrum of the irradiated enriched $^{44}\text{CaCO}_3$ -target material showed high radionuclide purity with less than 1% of the co-produced longer-lived $^{44\text{m}}\text{Sc}$ (γ -line of 271 keV) as the only by-product (Supplemental Fig. 1B). After 48 h (> 10 half-lives of ^{44}Sc) the γ -spectrum of the same aliquot showed only remaining $^{44\text{m}}\text{Sc}$ and its decay product ^{44}Sc which proved the excellent radiochemical purity (Supplemental Fig. 1C).

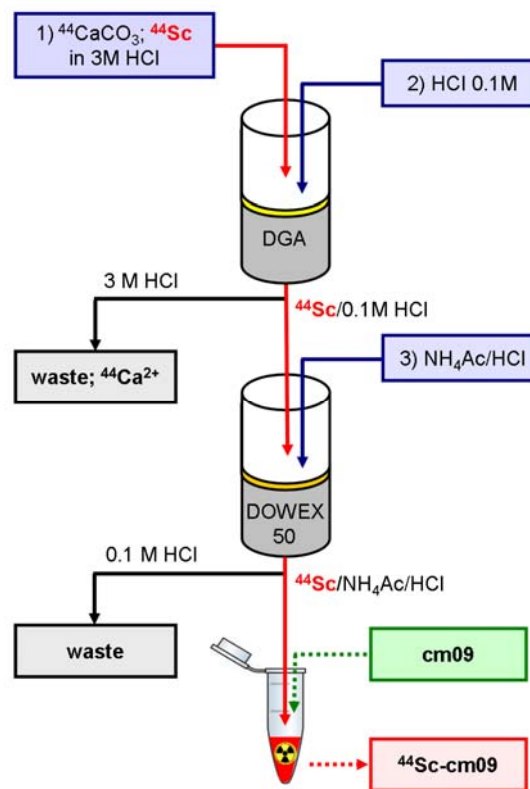
Based on these results it was concluded that the production of ^{44}Sc from enriched ^{44}Ca -targets is the preferred method. As mentioned above, ^{44}Sc which is produced from enriched ^{44}Ca -targets, is obtained in much higher radiochemical purity compared to ^{44}Sc produced from natural Ca-targets. A further advantage of using enriched ^{44}Ca -targets is the much lower amount of $^{44}\text{CaCO}_3$ (5-10 mg) which is required to obtain the same amount of ^{44}Sc as would be required if $^{\text{nat}}\text{CaCO}_3$ (200 mg) was irradiated. A smaller amount of CaCO_3 is more favorable with regard to the separation procedure of $^{44}\text{Sc(III)}$ from Ca(II) .



SUPPLEMENTAL FIGURE 1. (A) γ -Spectrum of a sample (1 mL) of irradiated $^{nat}\text{CaCO}_3$ target material dissolved in HCl (3 M) 5 h after end of beam. (B) γ -Spectrum of a sample (1 mL) of irradiated enriched $^{44}\text{CaCO}_3$ target material dissolved in HCl (3 M) 5 h after end of beam and (C) 48 h after end of irradiation.

2. Separation of ^{44}Sc from Irradiated ^{44}Ca -Targets

For separation of ^{44}Sc from irradiated ^{44}Ca -targets we developed a semi-automated separation system which was based on extraction chromatography and cation exchange chromatography. The experimental procedure is described in the main manuscript. A schematic illustration of the separation process is given in Supplemental Figure 2.



SUPPLEMENTAL FIGURE 2. Schematic illustration of the isolation of ^{44}Sc from proton-irradiated ^{44}Ca -targets (DGA = *N,N,N',N'*-tetra-*n*-octyldiglycolamide).

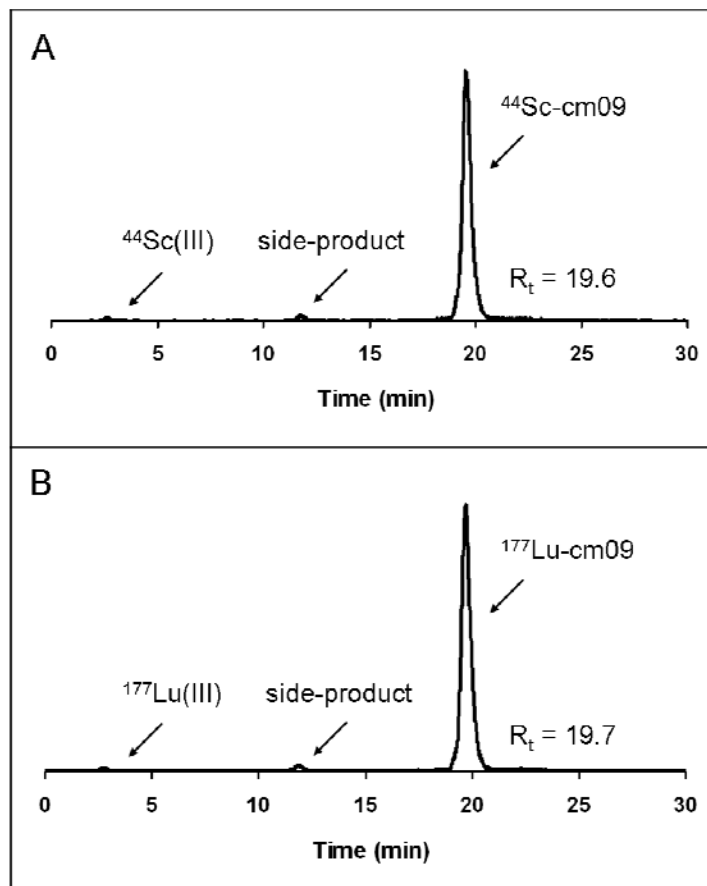
3. In Vitro Comparison of ^{44}Sc -cm09 and ^{177}Lu -cm09

Purpose. Formation of DOTA-complexes with $^{44}\text{Sc}(\text{III})$ and $^{177}\text{Lu}(\text{III})$ are supposed to occur according to the same coordination chemistry (5). In contrast to ^{68}Ga -DOTA-complexes, which differ significantly from ^{177}Lu -DOTA complexes, similar chemical characteristics of $^{44}\text{Sc}(\text{III})$ and $^{177}\text{Lu}(\text{III})$ would allow comparison of biomolecules labeled with either of these radioisotopes (6). In order to compare the characteristics of ^{44}Sc -cm09 with ^{177}Lu -cm09 we investigated the retention times of the compounds using the same HPLC method and determined the *n*-octanol/PBS distribution coefficients (LogD values). Both parameters are dependent on the hydrophilicity of a specific radioconjugate.

Experimental. High-performance liquid chromatography (HPLC) was performed using a C-18 reversed phase column (Xterra MS C18, 5 μm , 15 cm x 4.6 cm, Waters) with a mobile phase consisting of MilliQ water with 0.1 % trifluoroacetic acid (A) and methanol (B) with a linear gradient from 95% A and 5% B to 20% A and 80% B over 25 min and a flow rate of 1 mL/min. The experimental procedure for the determination of the logD value is reported in the main manuscript and in previous publications (7, 8).

Results and Conclusion of the In Vitro Comparison of ^{44}Sc -cm09 and ^{177}Lu -cm09. Representative HPLC chromatograms of ^{44}Sc -cm09 and ^{177}Lu -cm09 are shown in Supplemental Fig. 3. The retention time of ^{44}Sc -cm09 ($R_t = 19.6$ min, Supplemental Fig. 3A) was about the same as obtained for ^{177}Lu -cm09 ($R_t = 19.7$ min, Supplemental Fig. 3B). The logD value of ^{44}Sc -cm09 was -4.49 ± 0.12 as reported in the main manuscript. This value was similar to the logD value of ^{177}Lu -cm09 (-4.25 ± 0.41) (7).

These results indicate similar characteristics of ^{44}Sc -cm09 and ^{177}Lu -cm09 with regard to their hydrophilicity. These findings are in agreement with the theory of identical coordination chemistry among the two radioisotopes ^{44}Sc and ^{177}Lu .



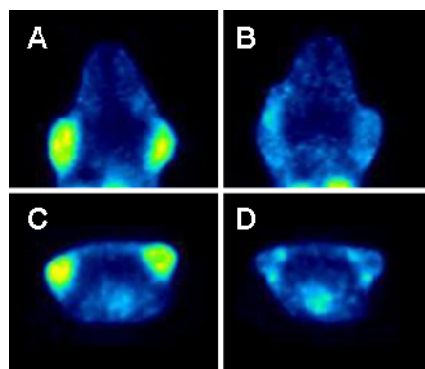
SUPPLEMENTAL FIGURE 3. Representative HPLC chromatograms of $^{44}\text{Sc-cm09}$ (A) and $^{177}\text{Lu-cm09}$ (B).

4. **Additional** PET Imaging Studies with $^{44}\text{Sc-cm09}$

Purpose. In order to investigate FR specific accumulation of $^{44}\text{Sc-cm09}$ in KB tumor xenografts, we also performed PET imaging studies with a tumor bearing mouse which was injected with excess folic acid prior to the radiotracer. It was expected that blockade of FRs by folic acid would result in a significant decline of $^{44}\text{Sc-cm09}$ uptake in the tumor tissue.

Experimental Procedure. Imaging studies were performed with nude mice ~ 14 days after KB tumor cell inoculation. $^{44}\text{Sc-cm09}$ (~ 25 MBq, ~ 6 nmol per mouse, 100 μL) was injected either as a single agent or immediately after injection of excess folic acid (100 μg in 100 μL PBS). PET scans of 30 min duration were performed with each of the two mice 4 h after injection of the radioconjugate.

Results and Conclusion of Additional PET Imaging Studies with $^{44}\text{Sc-cm09}$. PET images of a mouse which received folic acid prior to the injection of $^{44}\text{Sc-cm09}$ showed reduced uptake of radioactivity in the tumor xenografts compared to the tumor uptake of $^{44}\text{Sc-cm09}$ found in the mouse which received only $^{44}\text{Sc-cm09}$. These results confirmed FR specific uptake of $^{44}\text{Sc-cm09}$ since injection of excess folic acid blocked FRs and, hence, prevented uptake of $^{44}\text{Sc-cm09}$ (Supplemental Fig. 4).



SUPPLEMENTAL FIGURE 4. PET images as coronal (A, B) and transaxial sections (C, D) of KB tumor bearing mice injected with $^{44}\text{Sc-cm09}$ only (A, C) or with $^{44}\text{Sc-cm09}$ and preinjected folic acid to block FRs (B, D).

5. In Vivo Biodistribution Data of $^{177}\text{Lu-cm09}$

The tissue distribution data of $^{177}\text{Lu-cm09}$ in KB tumor bearing nude mice at different time points after injection are given in Supplemental Table 1.

SUPPLEMENTAL TABLE 1

Biodistribution of $^{177}\text{Lu-cm09}$ in KB Tumor Bearing Female Nude Mice (7).

	$^{177}\text{Lu-cm09}$			
	% injected dose per gram tissue*			
	1 h p.i.	2 h p.i.	4 h p.i.	24 h p.i.
Blood	8.15 ± 1.21	6.76 ± 0.95	4.38 ± 0.95	1.22 ± 0.19
Lung	4.58 ± 0.83	3.71 ± 0.65	2.70 ± 0.24	1.03 ± 0.20
Spleen	1.59 ± 0.25	1.50 ± 0.42	1.18 ± 0.19	0.63 ± 0.16
Kidneys	15.79 ± 2.13	23.23 ± 1.49	28.05 ± 1.35	30.09 ± 4.04
Stomach	2.04 ± 0.11	1.89 ± 0.59	1.45 ± 0.25	0.70 ± 0.14
Intestines	1.43 ± 0.31	1.07 ± 0.24	0.90 ± 0.20	0.29 ± 0.11
Liver	4.40 ± 0.14	3.98 ± 0.65	3.86 ± 0.65	1.80 ± 1.54
Salivary glands	6.78 ± 1.41	6.35 ± 1.05	6.23 ± 0.69	3.64 ± 0.49
Muscle	1.30 ± 0.06	1.31 ± 0.04	1.26 ± 0.06	0.96 ± 0.22
Bone	1.48 ± 0.08	1.49 ± 0.16	1.23 ± 0.14	0.62 ± 0.13
Tumor	10.84 ± 1.32	14.67 ± 1.65	18.12 ± 1.80	19.46 ± 3.13
Tumor-to-blood	1.36 ± 0.27	2.18 ± 0.18	4.32 ± 1.15	16.02 ± 1.52
Tumor-to-liver	2.47 ± 0.31	3.71 ± 0.30	4.73 ± 0.39	7.77 ± 0.62
Tumor-to-kidney	0.69 ± 0.04	0.63 ± 0.06	0.65 ± 0.07	0.65 ± 0.07

* values shown represent the mean ± S.D. of data from three animals (n=3) per cohort

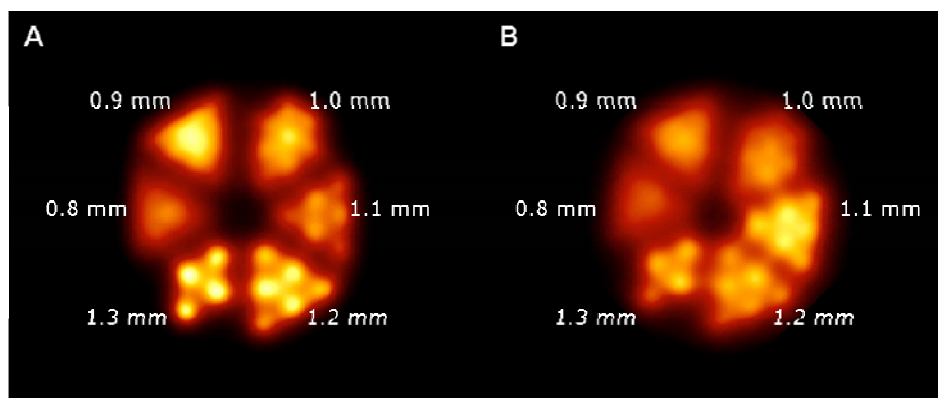
6. Comparison of ^{44}Sc and ^{68}Ga PET Using Derenzo Phantoms

Purpose. In order to investigate the resolution and PET image quality of ^{44}Sc and ^{68}Ga we performed a site-by-site comparison of these two radioisotopes using Derenzo phantoms and a small-animal PET scanner.

Experimental Procedure. PET scans of Derenzo phantoms were performed with a dedicated small-animal PET/CT camera (Vista eXplore, GE Healthcare). Two Derenzo phantoms with hole-diameters ranging from 0.8 to 1.3 mm, in 0.1-mm steps

were filled with ~ 9 MBq of $^{68}\text{Ga}(\text{III})$ and ~ 9 MBq of $^{44}\text{Sc}(\text{III})$, respectively, in a volume of 600 μL . Static PET scans of 30 min duration were acquired of each phantom. Reconstruction of PET data was performed using the instrument's software. For reconstruction, the 2-dimensional ordered-subset expectation maximization (2D-OSEM) algorithm was used.

Results and Conclusion Comparison of ^{44}Sc and ^{68}Ga PET Using Derenzo Phantoms. PET imaging of a Derenzo phantom filled with ^{44}Sc revealed an excellent resolution of ~1.2 mm (Supplemental Fig. 5A). These findings were similar or even superior to those obtained with an equivalent Derenzo phantom filled with about the same amount of ^{68}Ga -radioactivity (Supplemental Fig 5B).



SUPPLEMENTAL FIGURE 5. PET images of Derenzo phantoms. A: ^{44}Sc (~ 9 MBq, scan time: 30 min) and B: ^{68}Ga (~ 9 MBq, scan time: 30 min).

REFERENCES

1. Severin GW, Engle JW, Valdovinos HF, Barnhart TE, Nickles RJ. Cyclotron produced ^{44g}Sc from natural calcium. *Appl Radiat Isot.* 2012;70:1526-1530.
2. Krajewski S, Cydzik I, Abbas K, et al. Simple procedure of DOTATATE labelling with cyclotron produced ^{44}Sc and ^{43}Sc . *Nucl Med Rev.* 2012;15:A22-A46.
3. Kamel A, Izabela C, Federica S, Seweryn K, Agata K, Aleksander B. Cyclotron production of ^{44}Sc - new radionuclide for PET technique. *J Labelled Compd Rad.* 2011;54:S53-S53.
4. Zhernosekov K, Bunka M, Schibli R, Türler A. Development of ^{44}Sc production for radiopharmaceutical applications. *Radiother Oncol.* 2012;102:S141.
5. Viola-Villegas N, Doyle RP. The coordination chemistry of 1,4,7,10-tetraazacyclododecane-*N,N',N'',N'''*-tetraacetic acid (H_4DOTA): Structural overview and analyses on structure-stability relationships. *Coordin Chem Rev.* 2009;253:1906-1925.
6. Majkowska-Pilip A, Bilewicz A. Macrocyclic complexes of scandium radionuclides as precursors for diagnostic and therapeutic radiopharmaceuticals. *J Inorg Biochem.* 2011;105:313-320.
7. Müller C, Struthers H, Winiger C, Zhernosekov K, Schibli R. DOTA conjugate with an albumin-binding entity enables the first folic acid-targeted ^{177}Lu -radionuclide tumor therapy in mice. *J Nucl Med.* 2013;54:124-131.
8. Müller C, Mindt TL, de Jong M, Schibli R. Evaluation of a novel radiofolate in tumour-bearing mice: promising prospects for folate-based radionuclide therapy. *Eur J Nucl Med Mol Imaging.* Jun 2009;36:938-946.